

Article

Influence of the Chemical Composition on the Phase Stability and Mechanical Properties of Biomedical Ti-Nb-Mo-Zr Alloys

Aline Raquel Vieira Nunes ^{1,*}, Sinara Borborema ², Leonardo Sales Araújo ¹, Taissa Zangerolami Lopes Rodrigues ¹, Loïc Malet ³, Jean Dille ³ and Luiz Henrique de Almeida ¹

¹ Department of Metallurgical and Materials Engineering, Federal University of Rio de Janeiro, Rio de Janeiro 21941-599, RJ, Brazil; lsales@metalmat.ufrj.br (L.S.A.); taissazl@metalmat.ufrj.br (T.Z.L.R.); lha@metalmat.ufrj.br (L.H.d.A.)

² Department of Mechanical and Energy, Rio de Janeiro State University, Resende 27537-000, RJ, Brazil; sinara.borborema@fat.uerj.br

³ Engineering, Characterization, Synthesis and Recycling (4MAT), Université Libre de Bruxelles—ULB, 1050 Brussels, Belgium; loic.malet@ulb.be (L.M.); jean.dille@ulb.be (J.D.)

* Correspondence: alineraquel@metalmat.ufrj.br

Abstract: A new generation of titanium alloys with non-toxic, non-allergenic elements and lower Young's modulus (YM) have been developed, presenting modulus values close to that of bone. In titanium alloys, the value of the Young's modulus is strongly dependent on the chemical composition. Young's modulus also depends on the present phases and on the crystallographic texture related to the thermomechanical processing. A lower YM is normally attributed to the formation of the α'' phase into the β matrix, but there is no consensus for this assumption. In the present work, four alloys were designed and melted, based on the Ti-Nb-Mo-Zr system and heat-treated to favor the formation of the β phase. The alloys were produced by arc melting under argon atmosphere and heat-treated at 1000 °C for 24 h under high vacuum, being subsequently quenched in water to room temperature. Alloys were then characterized by optical microscopy (OM), X-ray diffraction (XRD) and transmission electron microscopy (TEM). Young's modulus was determined by the impulse excitation technique and Vickers microhardness. The purpose of the study was to define an optimal chemical composition for the further production on a semi-industrial scale of a new Ti-Nb-Mo-Zr alloy for orthopedic implant manufacturing. The results showed that all of the four studied alloys are potential candidates for biomedical applications. Among them, the Ti-24Nb-4Mo-6Zr alloy has the lowest Young's modulus and the highest microhardness. So, this alloy presents the highest HV/YM ratio, which is a key indicator in order to evaluate the mechanical performance of metallic biomaterials for orthopedic implants.

Keywords: titanium alloys; phase stability; microstructure; mechanical properties; metallic biomaterials



Citation: Nunes, A.R.V.; Borborema, S.; Araújo, L.S.; Rodrigues, T.Z.L.; Malet, L.; Dille, J.; de Almeida, L.H. Influence of the Chemical Composition on the Phase Stability and Mechanical Properties of Biomedical Ti-Nb-Mo-Zr Alloys. *Metals* **2023**, *13*, 1889. <https://doi.org/10.3390/met13111889>

Academic Editors: Yadir Torres Hernández and Erlin Zhang

Received: 18 September 2023

Revised: 1 November 2023

Accepted: 8 November 2023

Published: 14 November 2023



Copyright: © 2023 by the authors. Licensee MDPI, Basel, Switzerland. This article is an open access article distributed under the terms and conditions of the Creative Commons Attribution (CC BY) license (<https://creativecommons.org/licenses/by/4.0/>).

1. Introduction

Titanium and its alloys have been widely used as orthopedic implants, due to, among other properties, their low Young's modulus combined with high strength, when compared with other metallic biomaterials such as austenitic stainless steel and Co-Cr alloys [1–4]. While pure titanium presents a Young's modulus of around 105 GPa, the $\alpha + \beta$ alloys, such as Ti-6Al-4V, for example, exhibit Young's moduli ranging between 101 and 120 GPa. On the other hand, metastable β -type titanium alloys with biocompatible and non-cytotoxic elements, such as Nb, Mo, Ta, Zr and Sn, have been developed with lower Young's moduli and higher strength [5–7].

Several papers on the development of metastable β -type titanium alloys have been presented in the literature [8–11]. Most of these studies include the following systems: Ti-Mo, Ti-Nb, Ti-Nb-Zr, Ti-Mo-Nb, Ti-Nb-Mo-Zr, Ti-Sn-Nb-Ta, Ti-Zr-Nb-Ta and Ti-Nb-Ta-Mo, with Young's moduli ranging between 50 and 95 GPa, depending on the alloy's

chemical composition and on the final microstructure [12–14]. In these systems, a lower Young's modulus is normally attributed to the presence of the α'' phase in the β matrix while, in the opposite direction, the ω phase must be avoided [15–17]. However, there is no consensus on obtaining a low modulus in these alloys when processed for single β phase microstructure. Table 1 summarizes some relevant works with metastable β -type titanium alloys containing the elements Nb, Mo, Ta, Sn and Zr in their composition, outlining the present phases on the microstructure and mechanical properties.

Zirconium is a strong transition metal belonging to the same IVB group as titanium. This element exhibits chemical properties that are similar to that of titanium, besides being able to form solid solutions in titanium's hexagonal close-packed (HCP) and body-centered cubic (BCC) structure. Furthermore, its addition contributes to mechanical and corrosion resistances, as well as an increased biocompatibility with bodily fluids [18,19]. The overall contribution of alloying elements to the β stability is determined by the Mo equivalent method [20]. Often, Zr is considered a neutral element and is not taken into account in the Moeq formula. But, recently, the role of Zr has been investigated and included as a β phase stabilizer by a factor close to 0.3 [21–23]. In turn, molybdenum is a strong β -stabilizing element and may exhibit a wide composition range in which the α and β titanium phases can be present at room temperature [18]. Studies have shown that Mo, in addition to being a β stabilizer, strongly contributes to increased strength and a reduced Young's modulus [24,25]. Niobium is also a β -stabilizing element [26]. Titanium alloys with Nb contents up to 15 wt % present a hexagonal α' martensite phase after water quenching. For Nb contents between 17.5% and 25%, water quenching led to the development of the orthorhombic α'' phase. However, for Nb contents higher than 30%, the β phase is present in the microstructure of these rapidly cooled alloys [27–29].

A low Young's modulus is important for titanium alloys used in orthopedic implants such as hip prosthetic stems. This requirement is key to prevent the stress shielding that occurs due to the differences in Young's modulus between the prosthetic stem and the cortical bone. On the other hand, high strength is another important mechanical property for load-bearing orthopedic applications. The strength also determines the fatigue resistance of the material used as an implant that undergoes cyclic loading during its use in the human body. The strength of metallic alloys is often evaluated by hardness measurements. For this reason, the hardness-to-Young's-modulus ratio (H/YM) is used as an indicator to evaluate the quality of the mechanical performances of metallic biomaterials for implants [30].

Table 1. Influence of Nb, Mo and Zr elements on the microstructure and mechanical properties of some β -type titanium alloys.

Alloy	[Moeq] %	Alloy Manufacturing Route	σ_e (MPa)	YM (GPa)	Phases Present	Remarks	Ref.
Ti-6Mo	6	As cast	-	64 ⁽¹⁾	α''	The orthorhombic α'' phase Ti-7.5Mo alloy had the lowest YM of all the phases in the binary Ti-Mo system. Among all β phase alloys, Ti-10Mo had the highest YM and Ti-15Mo had the lowest.	[24]
Ti-7.5Mo	7.5		-	55 ⁽¹⁾	α''		
Ti-9Mo	9		-	75 ⁽¹⁾	$\beta + \alpha''$		
Ti-10Mo	10		-	95 ⁽¹⁾	β		
Ti-12.5Mo	12.5		-	82 ⁽¹⁾	β		
Ti-15Mo	15		-	71 ⁽¹⁾	β		
Ti-20Mo	20		-	85 ⁽¹⁾	β		
Ti-8Mo-6Nb-4Zr	9.68	ST (80% red.) + AT 950 °C/2 h + WQ	899	72 ⁽²⁾	β	A lower Nb content allowed α'' phase precipitation, as Nb acts as a β -stabilizer element. An increase in Zr favored a reduction in YM, besides a drop in TS as the Nb content decreased.	[31]
Ti-8Mo-5Nb-3Zr	9.40		947	69 ⁽²⁾	β		
Ti-8Mo-4Nb-5Zr	9.12		483	52 ⁽²⁾	$\beta + \alpha''$		
Ti-10Mo-3Nb	10.84	ST 950 °C/1 h + WQ	-	105 ⁽²⁾	β	In these alloys, an increase in Nb content favored an increase in YM, while no significant changes in hardness were observed.	[32]
Ti-10Mo-6Nb	11.68		-	122 ⁽²⁾	$\beta + \alpha' + \omega$		
Ti-10Mo-9Nb	12.52		-	120 ⁽²⁾	$\beta + \omega$		
Ti-10Mo	10	ST 850 °C + WQ	690	93 ⁽³⁾	$\beta + \omega$	After solubilization, an increase in Mo stabilized the β phase, although a reduction in TS and in YM were observed, probably due to the absence of the ω phase.	[33]
Ti-20Mo	20		428	75 ⁽³⁾	β		
Ti-25Nb	7	ST 950 °C/1 h + ice water	-	80 ⁽²⁾	α''	An increase in Nb favored a decrease in YM	[29]
Ti-30Nb	8.4		-	85 ⁽²⁾	$\beta + \alpha''$		
Ti-35Nb	9.8		-	72 ⁽²⁾	$\beta + \alpha''$		
Ti-40Nb	11.2		-	62 ⁽²⁾	$\beta + \alpha''$		
Ti-29Nb-13Ta	10.98	CR (75% red.) + AT 845 °C/30 min + WQ	250	64 ⁽³⁾	β	Zr favored a decrease in YM and an increase in TS.	[8]
Ti-29Nb-13Ta-4,6Zr	10.98		300	50 ⁽³⁾	β		
Ti-29Nb-13Ta-4Mo	14.98	CR (75% red.) + AT 845 °C/30 min + WQ	620	50 ⁽³⁾	β	An increase in Nb did not cause any significant changes in YM, though caused a slight increase in TS.	[8]
Ti-16Nb-13Ta-4Mo	11.34		590	47 ⁽³⁾	β		
Ti-29Nb-13Ta-4Mo	14.98		620	50 ⁽³⁾	β		
Ti-29Nb-13Ta-2Sn	10.98		450	47 ⁽³⁾	β		
Ti-29Nb-13Ta-4,6Zr	10.98	HF (850 °C) + AT 1000 °C/1 h + WQ + 260 °C/4 h + WQ	300	50 ⁽³⁾	β	Both alloys presented similar YM. Mo and Zr were efficient in reducing YM, Mo being more efficient in increasing TS.	[34]
Ti-29Nb-13Ta-4Mo	14.98		620	50 ⁽³⁾	β		
Ti-30Nb-2Sn	8.40	Cold Forging 90% Ti-32.5Nb-6.8Zr-2.7Sn-0.3O	500	65 ⁽²⁾	$\beta + \alpha''$	A higher Nb content favored a lower YM.	[35]
Ti-32.5Nb-6.8Zr-2.7Sn-0.3O	9.10		1093	54 ⁽³⁾	β		
Ti-33.6Nb-4Sn	9.41		40 ⁽³⁾	$\beta + \alpha''$			[36]
Ti-35Nb-5Ta-7Mo	17.9	ST 1000 °C/2 h + WQ	510	59 ⁽³⁾	β	An increase in Nb content to 35% and the presence of Mo favored a decrease in all mechanical properties.	[37]
Ti-32.5Nb-6.8Zr-2.7Sn-0.3O	9.10	ST 1000 °C/1 h + WQ	829	67 ⁽³⁾	β		

Young Modulus (YM), Tensile strength (TS), Solution treatment (ST), water quenching (WQ), cold rolling (CR), hot forging (HF), annealing treatment (AT). ⁽¹⁾ Bending test, ⁽²⁾ ultrasound, ⁽³⁾ tensile tests.

In the present work, four alloys were produced, based on the Ti-Nb-Mo-Zr system, with different chemical compositions but similar Moeq values, in order to obtain a single phase β in the solubilized condition. The samples were characterized by optical microscopy, transmission electron microscopy, X-ray diffraction, microhardness and Young's modulus measurement. The purpose of the study was to determine an optimal chemical composition for the further production on a semi-industrial scale of a new Ti-Nb-Mo-Zr alloy for orthopedic implant. The most promising alloy was determined by the highest hardness-to-Young's-modulus ratio.

2. Materials and Methods

Ingots of the Ti-29Nb-2Mo-3Zr, Ti-29Nb-2Mo-6Zr, Ti-24Nb-4Mo-3Zr and Ti-24Nb-4Mo-6Zr alloys were produced from commercially pure Ti (ASTM F67), Mo (>99.9%, Plansee Group, Austria), Nb (>99.9%, EEL/USP, Brazil) and Zr (Nuclear grade) by the arc melting process, with a tungsten electrode on a water-cooled copper crucible. The elements were weighed individually. Two ingots of each composition were prepared under a high-purity argon atmosphere (>99.9999% pure) and were then re-melted eight times to assure chemical composition homogeneity. The obtained ingots (60 g – 17 × 12 × 70 mm) were weighed, showing a mass loss < 1%, and finally solution-treated at 1000 °C under argon atmosphere for 24 h and then quenched in water at room temperature.

The chemical compositions of the studied alloys are mentioned in Table 2. These compositions were based on the phase stability diagram proposed by Abdel-Hady, related to the Bo/Md parameters [38], where Bo is the average bond order between atoms and Md is the average d-orbital energy level of the element in the alloy. They are also based on the molybdenum equivalence ([wt %Mo]eq), with 10% being the minimum value necessary to stabilize the β phase upon water quenching, according to Mythili et al. [20]. Jiang et al. [21,22] proposed a new Moeq formula including neutral elements such Zr and Sn: $(\text{Moeq})Q = 1.0 \text{ Mo} + 1.25 \text{ V} + 0.59 \text{ W} + 0.33 \text{ Nb} + 0.25 \text{ Ta} + 1.93 \text{ Fe} + 1.84 \text{ Cr} + 1.51 \text{ Cu} + 2.46 \text{ Ni} + 2.67 \text{ Co} + 2.26 \text{ Mn} + 0.30 \text{ Sn} + 0.31 \text{ Zr} + 3.01 \text{ Si} - 1.47 \text{ Al}$ (wt %). The number of valence electrons per atom (e/a) is another criterion used to analyze the β -phase stability and the precipitation of other phases. The results of e/a for the four alloys are also presented in Table 2, showing average e/a values between 4.19 and 4.20. The positions of the four alloys on the phase stability diagram are represented on Figure 1.

Table 2. Mass and atomic composition target, calculated parameters for Bo and Md, Mo equivalent [Moeq] and average number of valence electrons per atom for experimental alloys of the Ti-Nb-Mo-Zr system proposed in the present work.

Alloys Ident.	Alloys (% Mass)	Ti	Nb	Mo	Zr	Bo	Md	[Moeq] % [20]	[Moeq] % [21]	e/a
		% Atomic								
1	Ti-29Nb-2Mo-3Zr	79.03	17.89	1.19	1.88	2.854	2.446	10.12	12.50	4.203
2	Ti-29Nb-2Mo-6Zr	76.75	18.20	1.22	3.84	2.861	2.456	10.12	13.43	4.206
3	Ti-24Nb-4Mo-3Zr	81.24	14.56	2.35	1.85	2.847	2.441	10.72	12.85	4.193
4	Ti-24Nb-4Mo-6Zr	79.03	14.81	2.39	3.77	2.853	2.450	10.72	13.78	4.196

Phase identification was carried out by X-ray diffraction operated at 40 kV and 30 mA, using Ni-filtered CuK α radiation.

For optical microscopy (OM), the samples were mechanically polished and then etched with Kroll's reagent (8 mL HF, 20 mL HNO₃ and 62 mL H₂O). The grain size was measured from the optical micrographs using the Heyn intercept method and ImageJ software, available at: <https://imagej.net/ij/download.html>.

Transmission electron microscopy (TEM) thin foils were prepared by the focused ion beam technique and analyzed in a FEI CM20 electron microscope operating at 200 kV.

The Vickers microhardness HV was measured using a 200 gf load for 15 s. The presented values represent the average value of ten indentations. The Young's modulus

(YM) was determined by Impulse Excitation Technique by Sonelastic®, São Paulo, Brazil. Ten measurements were performed for each sample. For comparison purposes, the value of the Young's modulus of Ti-6Al-4V was also determined under the same conditions.

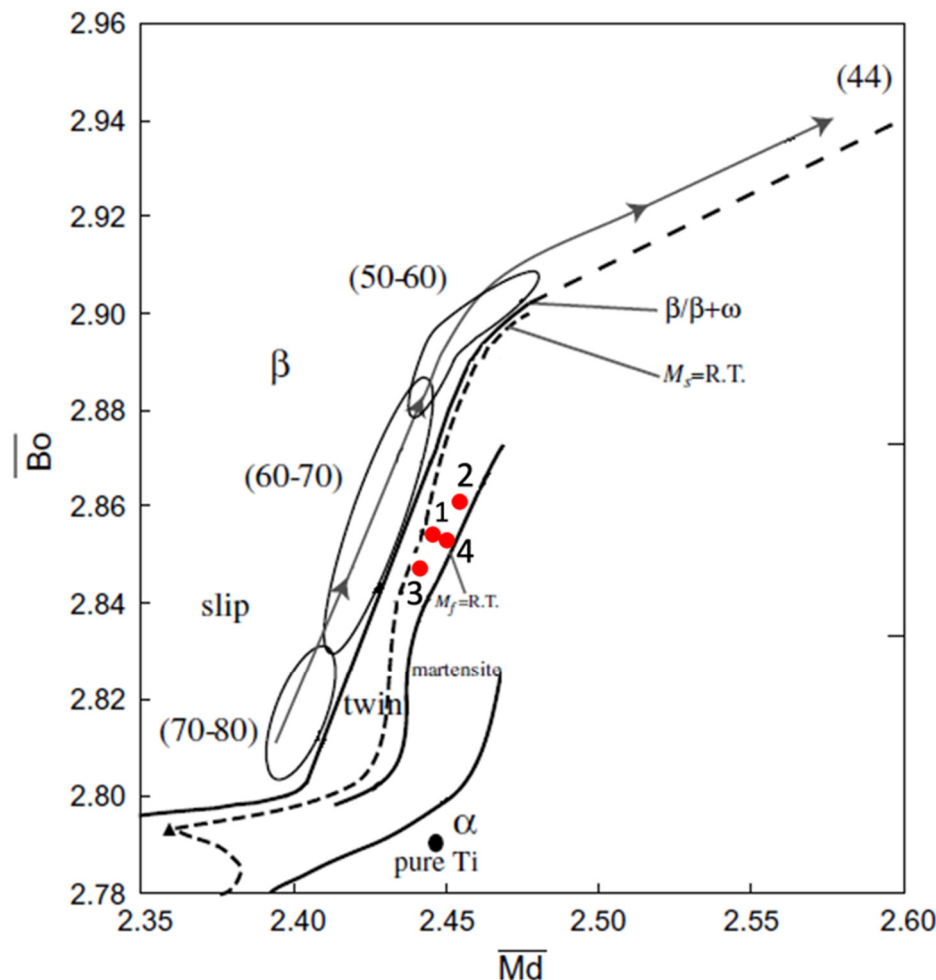


Figure 1. Phase stability diagram for Bo and Md parameters with Ti-Mo-Nb-Zr system alloys used in the present work (Reprinted with permission from Ref. [38]. Copyright 2006 Elsevier).

3. Results and Discussion

Figure 2 presents the microstructure observed by OM after solubilization followed by water quenching. For all micrographs, the single-phase microstructure is characterized by large and equiaxed grains. The measured grain size is approximately $910 \pm 166 \mu\text{m}$ and $925 \pm 170 \mu\text{m}$ in diameter for the samples with 3% of Zr, and approximately $590 \pm 136 \mu\text{m}$ and $650 \pm 115 \mu\text{m}$ in diameter for the samples with 6% Zr. Thus, smaller grains were observed in the alloys containing 6% Zr.

On Figure 3, the X-ray diffraction patterns reveal only the β phase in solubilized and water-quenched Ti-29Nb-2Mo-3Zr, Ti-29Nb-2Mo-6Zr and Ti-24Nb-4Mo-6Zr alloys. A small quantity of α'' martensite is also detected in Ti-24Nb-4Mo-3Zr alloy.

An increase in the Zr content led to the suppression of the α'' phase, as pointed out by Abdel-Hady [39] and Correa et al. [40], who highlighted that Zr tends to stabilize the β phase, even in small amounts, when acting in combination with another β -stabilizing element, such as Mo and Nb, even though it is considered a neutral element. For this reason, the α'' phase is not observed in Ti-24Nb-4Mo-6Zr alloy.

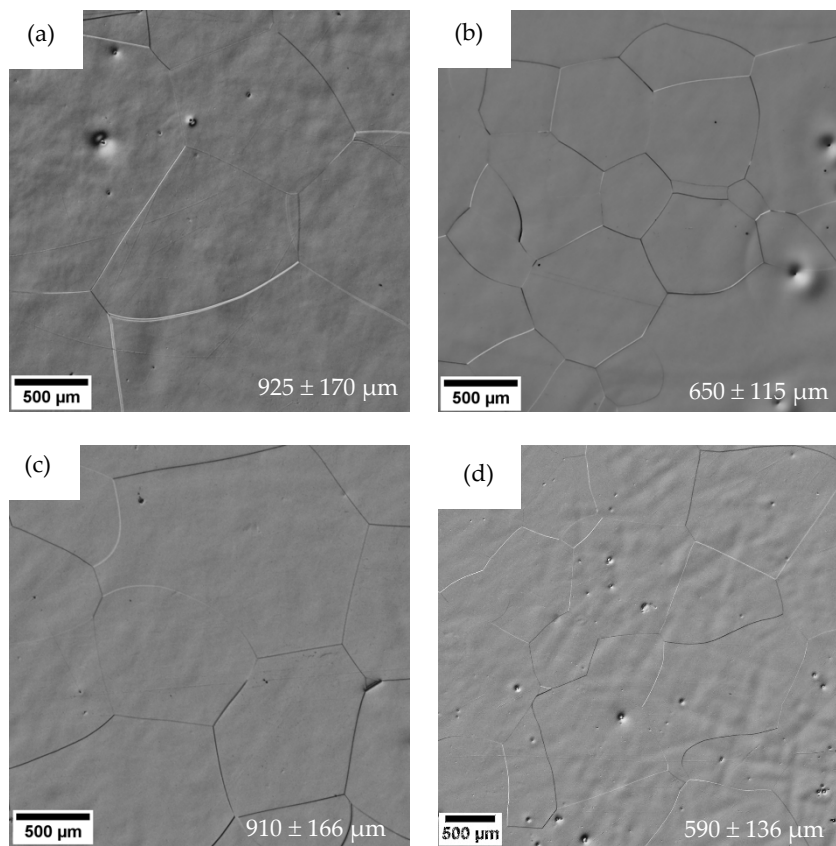


Figure 2. Optical micrographs (OM) for alloys (a) Ti-29Nb-2Mo-3Zr, (b) Ti-29Nb-2Mo-6Zr, (c) Ti-24Nb-4Mo-3Zr and (d) Ti-24Nb-4Mo-6Zr solubilized at 1000 °C for 24 h and water-quenched. Grain size values are indicated for each sample. Kroll attack.

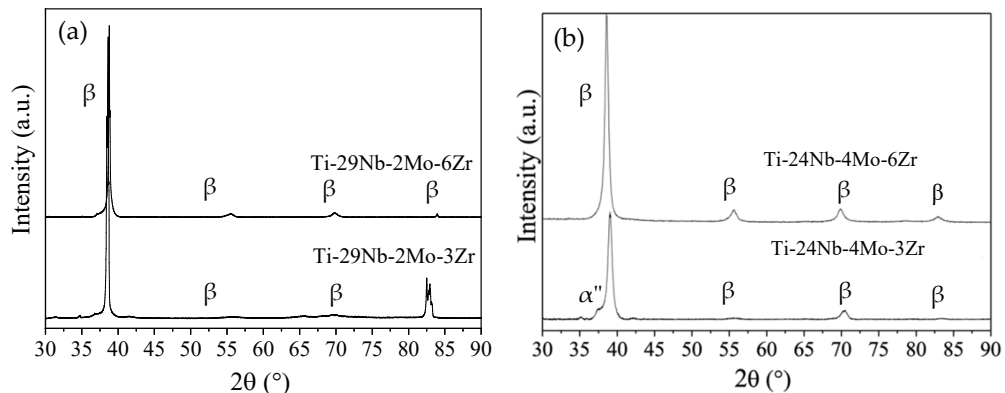


Figure 3. XRD patterns of the alloys (a) Ti-29Nb-2Mo-3Zr and Ti-29Nb-2Mo-6Zr, and (b) Ti-24Nb-4Mo-3Zr and Ti-24Nb-4Mo-6Zr solubilized at 1000 °C for 24 h and water-quenched.

On the other hand, the α'' phase could also be formed by deformation during mechanical polishing before XRD analysis. In any case, it is reasonable to consider that the influence of the small quantity of α'' phase in Ti-24Nb-4Mo-3Zr alloy on the mechanical properties is negligible.

Transmission electron microscopy also reveals the presence of nanosized athermal ω precipitates (in black) inside the β matrix, as shown on Figure 4a. The selected area electron diffraction pattern of Figure 4b corresponds to the $[311]_{\beta}$ zone axis. Sharp spots at $1/3$ and $2/3 <112>_{\beta}$ are attributed to ω phase. The dark-field image shown in Figure 4c and taken from the ω diffraction spots inside the red circle on Figure 4b confirms the athermal ω precipitation during the quench.

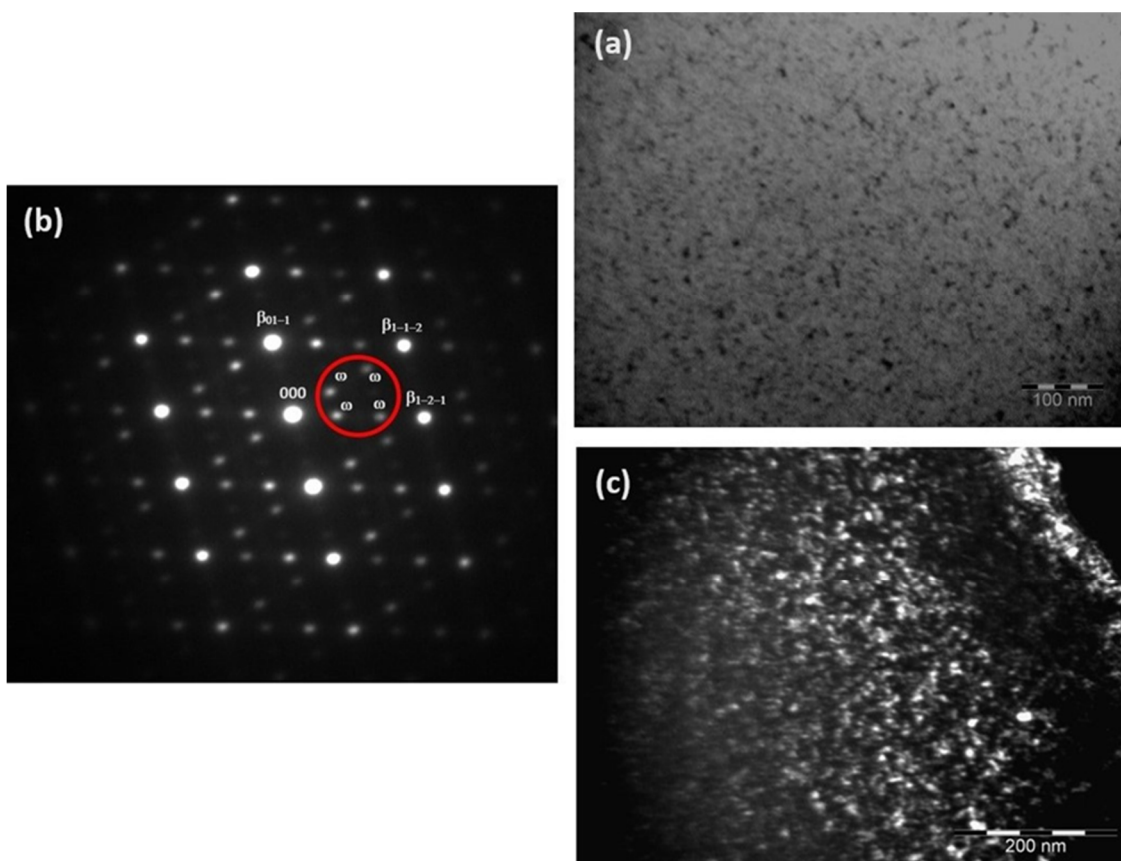


Figure 4. TEM analysis of Ti-24Nb-4Mo-3Zr alloy. (a) TEM bright-field image. (b) selected area electron diffraction pattern from the region shown on Figure 3a. (c) dark-field image taken from the red circle on Figure 3b.

In this study, athermal ω phase has been detected in samples containing 3% Zr as well as in samples containing 6% Zr. A study of Nejedzchlebova et al. concluded that athermal ω precipitation only negligibly affects the elastic constants [41] while Ho reports an increase in microhardness associated with the presence of athermal ω [42].

Table 3 presents the results of Vickers microhardness and Young's modulus, as well as the microhardness/Young's modulus ratio measured for the 4 experimental alloys. For comparison, the table also presents the mechanical properties of commercial Ti-6Al-4V alloy.

Table 3. Vickers microhardness (HV 0.2), Young's modulus (YM) and HV/YM ratio of solution-treated alloys at 1000 °C for 24 h and water-quenched.

Alloy	Hardness (HV-0.2)	YM (GPa)	HV/YM
Ti-29Nb-2Mo-3Zr	212.2 ± 7.0	64 ± 2.0	3.31
Ti-29Nb-2Mo-6Zr	228.4 ± 5.6	62 ± 2.0	3.65
Ti-24Nb-4Mo-3Zr	235.2 ± 4.8	60 ± 1.0	3.92
Ti-24Nb-4Mo-6Zr	244.8 ± 9.0	56 ± 1.0	4.37
Ti-6Al-4V	338 ± 6.0	118 ± 1.0	2.89

For solubilized β -Ti alloys, weakly textured, the main factor influencing Young's modulus is the chemical composition of the alloy. Indeed, elastic moduli are fundamentally connected to the interatomic bond forces. Chemical composition also influences microhardness due to solid solution hardening.

For the 4 studied alloys, Table 3 indicates that for a given value of Zr content, a simultaneous increase in Nb content with a decrease in Mo content leads to an increase in Young's modulus together with a decrease of microhardness. On the other hand, for given values of Nb and Mo content, an increase in Zr content induces a decrease in Young's modulus and an increase in microhardness.

In each case, Young's modulus and microhardness evolve in opposite ways. This is contrary to the global evolution of Young's modulus with regard to microhardness, which vary in the same direction for Ti-Nb-Mo-Zr alloys [43]. In fact, it is difficult to define a direct relationship between mechanical properties and chemical composition for a quaternary alloy, as it involves complex interactions between the elements.

Nevertheless, the results mentioned in Table 3 corroborate several previous studies on binary or ternary β -Ti alloys:

- Young's modulus decreases with an increase in Mo%, as observed by Li et al. [44] in Ti-26Nb-xMo alloys ($x = 0, 2, 4, 6$ and 8 wt %).
- Following Kim et al. [45], Young's modulus gradually decreases with decreasing Nb content from 29 wt % to 24 wt % for both Ti-xNb-4Zr and Ti-xNb-8Zr alloys.
- As reported by Tan et al. [46], microhardness decreases when Nb content increases from 23 wt % to 33 wt % in Ti-xNb-7Zr alloys.
- Chui et al. [4] investigated Ti-Zr-Nb-Mo alloys and also measured an increase in microhardness with increasing Mo content.
- In the same way, Ning et al. [47] concluded that an increase in Zr content reduces the elastic modulus of Ti-35Nb-xZr alloys ($0 \leq x \leq 10$ wt %).

The results compiled in Table 3 indicate that all the 4 alloys in the solubilized state have a Young's modulus between 56 GPa and 64 GPa, which is lower than the Young's modulus measured on the Ti-6Al-4V alloy (118 GPa), used for comparison. Therefore, they all can be considered as potential materials for orthopedic implants.

On the other hand, the hardness of the Ti-Nb-Mo-Zr alloys is lower than the hardness of Ti-6Al-4V alloy. The studied alloys with a single β phase microstructure, with large grain size, present a lower strength than the bi-phased ($\alpha + \beta$) Ti-6Al-4V, in which the high number of α/β interfaces act as dislocation barriers, increasing the strength. The high strength is an important mechanical property for load-bearing orthopedic applications. From this point of view, several studies have been undertaken to improve the strength of metastable β -type Ti alloys [48–50]. The most efficient strengthening mechanism in these alloys is through aging heat treatments that lead to the precipitation of nanosized ω and/or α particles. However, in this study, the athermal omega phase detected by transmission electron microscopy had only a limited influence on the hardness of the alloys.

Considering the H/YM ratio as the main indicator to evaluate the mechanical performance of metallic biomaterials, this parameter is higher for all the Ti-Nb-Mo-Zr alloys than for the reference Ti-6Al-4V, making them preferable. Consequently, all designed alloys are promising candidates for biomedical applications.

Among them, the Ti-24Nb-4Mo-6Zr alloy has the lowest Young's modulus and the highest microhardness, consequently having highest HV/YM ratio. It corresponds to the optimal chemical composition for the further production on a semi-industrial scale of a new Ti-Nb-Mo-Zr alloy for orthopedic implants.

4. Conclusions

Four Ti-Nb-Mo-Zr b-metastable Ti alloys were studied to evaluate their mechanical performances for potential use as orthopedic implants. In the solubilized conditions, their microstructure consisted of large β grains. Fine athermal ω precipitates were also observed by transmission electron microscopy.

As a consequence of the chemical composition on the properties of the Ti-Nb-Mo-Zr alloys, they have a much lower Young's modulus and a higher HV/YM ratio when compared with the commercial Ti-6Al-4V alloy. Therefore, all the alloys can be considered as potential candidates for biomedical applications.

Nevertheless, they exhibit a lower hardness due to their large grained single β phase structure. In the bi-phased ($\alpha + \beta$) Ti-6Al-4V alloy, the high number of α/β interfaces act as dislocation barriers and increase the strength.

Among the studied alloys, Ti-24Nb-4Mo-6Zr had the lowest Young's modulus and the highest microhardness, and consequently the highest HV/YM ratio, which is a key indicator to evaluate the mechanical performance of metallic biomaterials for orthopedic implants.

Author Contributions: Conceptualization, A.R.V.N., S.B., L.S.A., J.D. and L.H.d.A.; Methodology, A.R.V.N., S.B. and L.H.d.A.; Formal analysis, A.R.V.N., L.S.A. and J.D.; Investigation, A.R.V.N.; Resources, L.H.d.A.; Writing—original draft, A.R.V.N.; Writing—review & editing, J.D. and L.H.d.A.; Visualization, A.R.V.N., S.B., T.Z.L.R. and L.M.; Supervision, L.H.d.A.; Funding acquisition, L.H.d.A. All authors have read and agreed to the published version of the manuscript.

Funding: This research was funded by Brazilian agencies CNPq (grants #161842/2015-1 and #204566/2018-5) and FAPERJ (grants # 205.714/2022 and 205.715/2022).

Data Availability Statement: The data of this study are available from the corresponding author. The data are not publicly available due to the fact that is an ongoing research and may be part of a patent application.

Conflicts of Interest: The authors declare no conflict of interest.

References

1. Mohammed, M.T.; Khan, Z.A.; Siddiquee, A.N. Beta titanium alloys: The lowest elastic modulus for biomedical applications: A review. *Int. J. Chem.* **2014**, *8*, 822–827.
2. Yao, T.T.; Zhang, Y.G.; Yang, L.; Bu, Z.Q.; Li, J.F. A Metastable Ti-Zr-Nb-Al Multi-Principal-Element Alloy with High Tensile Strength and Ductility. *Mater. Sci. Eng. A* **2022**, *851*, 143646. [[CrossRef](#)]
3. Stráský, J.; Preisler, D.; Seiner, H.; Bodnárová, L.; Janovská, M.; Košutová, T.; Harcuba, P.; Šalata, K.; Halmešová, K.; Džugan, J.; et al. Achieving High Strength and Low Elastic Modulus in Interstitial Biomedical Ti-Nb-Zr-O Alloys through Compositional Optimization. *Mater. Sci. Eng. A* **2022**, *839*, 142833. [[CrossRef](#)]
4. Chui, P.; Jing, R.; Zhang, F.; Li, J.; Feng, T. Mechanical Properties and Corrosion Behavior of β -Type Ti-Zr-Nb-Mo Alloys for Biomedical Application. *J. Alloys Compd.* **2020**, *842*, 155693. [[CrossRef](#)]
5. Lee, T.; Lee, S.; Kim, I.S.; Moon, Y.H.; Kim, H.S.; Park, C.H. Breaking the Limit of Young's Modulus in Low-Cost Ti-Nb-Zr Alloy for Biomedical Implant Applications. *J. Alloys Compd.* **2020**, *828*, 154401. [[CrossRef](#)]
6. Pilz, S.; Gustmann, T.; Günther, F.; Zimmermann, M.; Kühn, U.; Gebert, A. Controlling the Young's Modulus of a β -Type Ti-Nb Alloy via Strong Texturing by LPBF. *Mater. Des.* **2022**, *216*, 110516. [[CrossRef](#)]
7. Frutos, E.; Karlık, M.; Jiménez, J.A.; Langhansová, H.; Lieskovská, J.; Polcar, T. Development of New β/A'' -Ti-Nb-Zr Biocompatible Coating with Low Young's Modulus and High Toughness for Medical Applications. *Mater. Des.* **2018**, *142*, 44–55. [[CrossRef](#)]
8. Kuroda, D.; Niinomi, M.; Morinaga, M.; Kato, Y.; Yashiro, T. Design and Mechanical Properties of New β Type Titanium Alloys for Implant Materials. *Mater. Sci. Eng. A* **1998**, *243*, 244–249. [[CrossRef](#)]
9. Nunes, A.R.V.; Borborema, S.; Araújo, L.S.; Dille, J.; Malet, L.; de Almeida, L.H. Production, Microstructure and Mechanical Properties of Cold-Rolled Ti-Nb-Mo-Zr Alloys for Orthopedic Applications. *J. Alloys Compd.* **2018**, *743*, 141–145. [[CrossRef](#)]
10. Weng, W.; Biesiekierski, A.; Lin, J.; Ozan, S.; Li, Y.; Wen, C. Development of Beta-Type Ti-Nb-Zr-Mo Alloys for Orthopedic Applications. *Appl. Mater. Today* **2021**, *22*, 100968. [[CrossRef](#)]
11. Wu, J.; Tan, X.; An, X.; Zhang, J.; Guo, Y.; Liu, J.; Luo, Y.; Yao, W.; Kong, Q.; Wang, Q. Development of Biomedical Ti-Nb-Zr-Mn Alloys with Enhanced Mechanical Properties and Corrosion Resistance. *Mater. Today Commun.* **2022**, *30*, 103027. [[CrossRef](#)]
12. Abdel-Hady Gepreel, M.; Niinomi, M. Biocompatibility of Ti-Alloys for Long-Term Implantation. *J. Mech. Behav. Biomed. Mater.* **2013**, *20*, 407–415. [[CrossRef](#)] [[PubMed](#)]
13. Nunes, A.R.V.; Borborema, S.; Araújo, L.S.; de Almeida, L.H.; Kaufman, M.J. Production of a Novel Biomedical β -Type Titanium Alloy Ti-23.6Nb-5.1Mo-6.7Zr with Low Young's Modulus. *Metals* **2022**, *12*, 1588. [[CrossRef](#)]
14. Hanada, S.; Masahashi, N.; Semboshi, S.; Jung, T.K. Low Young's Modulus of Cold Groove-Rolled β Ti-Nb-Sn Alloys for Orthopedic Applications. *Mater. Sci. Eng. A* **2021**, *802*, 140645. [[CrossRef](#)]
15. Hanada, S.; Masahashi, N.; Jung, T.K. Effect of Stress-Induced A'' Martensite on Young's Modulus of β Ti-33.6Nb-4Sn Alloy. *Mater. Sci. Eng. A* **2013**, *588*, 403–410. [[CrossRef](#)]
16. Jung, T.K.; Lee, H.S.; Semboshi, S.; Masahashi, N.; Abumiya, T.; Hanada, S. A New Concept of Hip Joint Stem and Its Fabrication Using Metastable TiNbSn Alloy. *J. Alloys Compd.* **2012**, *536*, S582–S585. [[CrossRef](#)]
17. Hanada, S.; Masahashi, N.; Jung, T.K.; Miyake, M.; Sato, Y.S.; Kokawa, H. Effect of Swaging on Young's Modulus of β Ti-33.6Nb-4Sn Alloy. *J. Mech. Behav. Biomed. Mater.* **2014**, *32*, 310–320. [[CrossRef](#)]

18. Leyens, C.; Peters, M. *Titanium and Titanium Alloys—Fundamentals and Applications*; DLR—German Aerospace Center—Institute of Materials Research, Wiley: Köln, Germany, 2003; ISBN 3527305343.
19. Chen, G.; Xiao, Y.; Ji, X.; Liang, X.; Hu, Y.; Cai, Z.; Liu, J.; Tong, Y. Effects of Zr Content on the Microstructure and Performance of TiMoNbZrx High-Entropy Alloys. *Metals* **2021**, *11*, 1315. [[CrossRef](#)]
20. Mythili, R.; Paul, V.T.; Saroja, S.; Vijayalakshmi, M.; Raghunathan, V.S. Study of Transformation Behavior in a Ti-4.4 Ta-1.9 Nb Alloy. *Mater. Sci. Eng. A* **2005**, *390*, 299–312. [[CrossRef](#)]
21. Jiang, B.; Wang, Q.; Wen, D.; Xu, F.; Chen, G.; Dong, C.; Sun, L.; Liaw, P.K. Effects of Nb and Zr on Structural Stabilities of Ti-Mo-Sn-Based Alloys with Low Modulus. *Mater. Sci. Eng. A* **2017**, *687*, 1–7. [[CrossRef](#)]
22. Wang, Q.; Dong, C.; Liaw, P.K. Structural Stabilities of β -Ti Alloys Studied Using a New Mo Equivalent Derived from $[\beta / (\alpha + \beta)]$ Phase-Boundary Slopes. *Metall. Mater. Trans. A Phys. Metall. Mater. Sci.* **2015**, *46*, 3440–3447. [[CrossRef](#)]
23. Sidhu, S.S.; Singh, H.; Gepreel, M.A.H. A Review on Alloy Design, Biological Response, and Strengthening of β -Titanium Alloys as Biomaterials. *Mater. Sci. Eng. C* **2021**, *121*, 111661. [[CrossRef](#)] [[PubMed](#)]
24. Ho, W.F.; Ju, C.P.; Lin, J.H.C. Structure and Properties of Cast Binary Ti–Mo Alloys. *Biomaterials* **1999**, *20*, 2115–2122. [[CrossRef](#)] [[PubMed](#)]
25. Li, S.J.; Yang, R.; Li, S.; Hao, Y.L.; Cui, Y.Y.; Niinomi, M.; Guo, Z.X. Wear Characteristics of Ti-Nb-Ta-Zr and Ti-6Al-4V Alloys for Biomedical Applications. *Wear* **2004**, *257*, 869–876. [[CrossRef](#)]
26. Borborema, S.; de Holanda Ferrer, V.; Rocha, A.d.C.; Cossú, C.M.F.A.; Nunes, A.R.V.; Nunes, C.A.; Malet, L.; de Almeida, L.H. Influence of Nb Addition on α'' and ω Phase Stability and on Mechanical Properties in the Ti-12Mo-XNb Stoichiometric System. *Metals* **2022**, *12*, 1508. [[CrossRef](#)]
27. Lee, C.M.; Ju, C.P.; Chern Lin, J.H. Structure-Property Relationship of Cast Ti-Nb Alloys. *J. Oral Rehabil.* **2002**, *29*, 314–322. [[CrossRef](#)]
28. Yao, Q.; Sun, J.; Xing, H.; Guo, W.Y. Influence of Nb and Mo Contents on Phase Stability and Elastic Property of β -Type Ti-X Alloys. *Trans. Nonferrous Met. Soc. China* **2007**, *17*, 1417–1421. [[CrossRef](#)]
29. Mantani, Y.; Tajima, M. Effect of Ageing on Internal Friction and Elastic Modulus of Ti-Nb Alloys. *Mater. Sci. Eng. A* **2006**, *442*, 409–413. [[CrossRef](#)]
30. Vieira Nunes, A.R.; Borborema, S.; Araújo, L.S.; Malet, L.; Dille, J.; Henrique de Almeida, L. Influence of Thermo-Mechanical Processing on Structure and Mechanical Properties of a New Metastable β Ti-29Nb-2Mo-6Zr Alloy with Low Young's Modulus. *J. Alloys Compd.* **2020**, *820*, 153078. [[CrossRef](#)]
31. Nhamchi, P.S.; Obayi, C.S.; Todd, I.; Rainforth, M.W. Mechanical and Electrochemical Characterisation of New Ti-Mo-Nb-Zr Alloys for Biomedical Applications. *J. Mech. Behav. Biomed. Mater.* **2016**, *60*, 68–77. [[CrossRef](#)]
32. Gabriel, S.B.; Dille, J.; Nunes, C.A.; Soares, G.D.A. The Effect of Niobium Content on the Hardness and Elastic Modulus of Heat-Treated Ti-10Mo-XNb Alloys. *Mater. Res.* **2010**, *13*, 333–337. [[CrossRef](#)]
33. Zhou, Y.L.; Luo, D.M. Microstructures and Mechanical Properties of Ti-Mo Alloys Cold-Rolled and Heat Treated. *Mater. Charact.* **2011**, *62*, 931–937. [[CrossRef](#)]
34. Lopes, E.S.N.; Contieri, R.J.; Button, S.T.; Caram, R. Femoral Hip Stem Prosthesis Made of Graded Elastic Modulus Metastable β Ti Alloy. *Mater. Des.* **2015**, *69*, 30–36. [[CrossRef](#)]
35. Lan, C.; Wu, Y.; Guo, L.; Chen, F. Effects of Cold Rolling on Microstructure, Texture Evolution and Mechanical Properties of Ti-32.5Nb-6.8Zr-2.7Sn-0.3O Alloy for Biomedical Applications. *Mater. Sci. Eng. A* **2017**, *690*, 170–176. [[CrossRef](#)]
36. Hanada, S.; Masahashi, N.; Jung, T.K.; Yamada, N.; Yamako, G.; Itoi, E. Fabrication of a High-Performance Hip Prosthetic Stem Using β Ti-33.6Nb-4Sn. *J. Mech. Behav. Biomed. Mater.* **2014**, *30*, 140–149. [[CrossRef](#)] [[PubMed](#)]
37. Choe, H.C.; Saji, V.S.; Ko, Y.M. Mechanical Properties and Corrosion Resistance of Low Rigidity Quaternary Titanium Alloy for Biomedical Applications. *Trans. Nonferrous Met. Soc. China* **2009**, *19*, 862–865. [[CrossRef](#)]
38. Abdel-Hady, M.; Hinoshita, K.; Morinaga, M. General Approach to Phase Stability and Elastic Properties of β -Type Ti-Alloys Using Electronic Parameters. *Scr. Mater.* **2006**, *55*, 477–480. [[CrossRef](#)]
39. Abdel-Hady, M.; Fuwa, H.; Hinoshita, K.; Kimura, H.; Shinzato, Y.; Morinaga, M. Phase Stability Change with Zr Content in β -Type Ti-Nb Alloys. *Scr. Mater.* **2007**, *57*, 1000–1003. [[CrossRef](#)]
40. Correa, D.R.N.; Vicente, F.B.; Araújo, R.O.; Lourenço, M.L.; Kuroda, P.A.B.; Buzalaf, M.A.R.; Grandini, C.R. Effect of the Substitutional Elements on the Microstructure of the Ti-15Mo-Zr and Ti-15Zr-Mo Systems Alloys. *J. Mater. Res. Technol.* **2015**, *4*, 180–185. [[CrossRef](#)]
41. Nejezchlebová, J.; Janovská, M.; Seiner, H.; Sedlák, P.; Landa, M.; Šmilauerová, J.; Stráský, J.; Harcuba, P.; Janeček, M. The Effect of Athermal and Isothermal ω Phase Particles on Elasticity of β -Ti Single Crystals. *Acta Mater.* **2016**, *110*, 185–191. [[CrossRef](#)]
42. Ho, W.-F. Effect of Omega Phase on Mechanical Properties of Ti-Mo Alloys for Biomedical Applications. *J. Med. Biol. Eng.* **2008**, *28*, 47–51.
43. Ling, J.; Huang, D.; Bai, K.; Li, W.; Yu, Z.; Chen, W. High-Throughput Development and Applications of the Compositional Mechanical Property Map of the β Titanium Alloys. *J. Mater. Sci. Technol.* **2021**, *71*, 201–210. [[CrossRef](#)]
44. Li, P.; Ma, X.; Tong, T.; Wang, Y. Microstructural and Mechanical Properties of β -Type Ti–Mo–Nb Biomedical Alloys with Low Elastic Modulus. *J. Alloys Compd.* **2020**, *815*, 152412. [[CrossRef](#)]
45. Kim, K.M.; Kim, H.Y.; Miyazaki, S. Effect of Zr Content on Phase Stability, Deformation Behavior, and Young's Modulus in Ti-Nb-Zr Alloys. *Materials* **2020**, *13*, 476. [[CrossRef](#)] [[PubMed](#)]

46. Tan, M.H.C.; Baghi, A.D.; Ghomashchi, R.; Xiao, W.; Oskouei, R.H. Effect of Niobium Content on the Microstructure and Young's Modulus of Ti-XNb-7Zr Alloys for Medical Implants. *J. Mech. Behav. Biomed. Mater.* **2019**, *99*, 78–85. [[CrossRef](#)]
47. Ning, C.; Ding, D.; Dai, K.; Zhai, W.; Chen, L. The Effect of Zr Content on the Microstructure, Mechanical Properties and Cell Attachment of Ti-35Nb-XZr Alloys. *Biomed. Mater.* **2010**, *5*, 45006. [[CrossRef](#)]
48. Yumak, N.; Aslantas, K. A Review on Heat Treatment Efficiency in Metastable b Titanium Alloys: The Role of Treatment Process and Parameters. *J. Mater. Res. Technol.* **2020**, *9*, 15360–16280. [[CrossRef](#)]
49. Pilz, S.; Hariharan, A.; Günther, F.; Zimmermann, M.; Gebert, A. Influence of Isothermal Omega Precipitation Aging on Deformation Mechanisms and Mechanical Properties of a β -Type Ti-Nb Alloy. *J. Alloys Compd.* **2023**, *930*, 167309. [[CrossRef](#)]
50. Guo, Y.; Wei, S.; Yang, S.; Ke, Y.; Zhang, X.; Zhou, K. Precipitation Behavior of ω Phase and $\Omega \rightarrow \alpha$ Transformation in near β Ti-5al-5mo-5v-1cr-1fe Alloy during Aging Process. *Metals* **2021**, *11*, 273. [[CrossRef](#)]

Disclaimer/Publisher's Note: The statements, opinions and data contained in all publications are solely those of the individual author(s) and contributor(s) and not of MDPI and/or the editor(s). MDPI and/or the editor(s) disclaim responsibility for any injury to people or property resulting from any ideas, methods, instructions or products referred to in the content.